Mechanism of dehydroxylation temperature decrease and high temperature phase transition of coal-bearing strata kaolinite intercalated by potassium acetate

Hongfei Cheng [a,b], Qinfu Liu [a*], Xiaonan Cui [a], Qian Zhang [c], Zhiliang Zhang [a], Ray L. Frost [b•]

[a] *School of Geoscience and Surveying Engineering, China University of Mining & Technology, Beijing, 100083 China*

[b] *Chemistry Discipline, Faculty of Science and Technology, Queensland University of Technology, 2 George Street, GPO Box 2434, Brisbane, Queensland 4001, Australia*

[c] *School of Materials Science and Engineering, Henan Polytechnic University, Jiaozuo 454000, China*

Abstract

The thermal decomposition and dehydroxylation process of coal-bearing strata kaolinite-potassium acetate intercalation complex (CSKK) has been studied using X-ray diffraction (XRD), infrared spectroscopy (IR), thermal analysis, mass spectrometric analysis and infrared emission spectroscopy. The XRD results showed that the potassium acetate (KAc) have been successfully intercalated into coal-bearing strata kaolinite with an obvious basal distance increase of the first basal peak, and the positive correlation was found between the concentration of intercalation regent KAc and the degree of intercalation. As the temperature of the system is raised, the formation of $KHCO_3$, KCO_3 and $KAlSiO_4$, which is derived from the thermal decomposition or phase transition of CSKK, is observed in sequence. The IR results showed that new bands appeared, the position and intensities shift can also be found when the concentration of intercalation agent is raised. The thermal analysis and mass spectrometric analysis results revealed that CSKK is stable below 300 °C, and the thermal decomposition products (H_2O and CO_2) were further proved by the mass spectrometric analysis. A comparison of thermal analysis results of original coal-bearing strata kaolinite and its intercalation complex gives new discovery that not only a new mass loss peak is observed at 285 °C, but also the temperature of dehydroxylation and dehydration of coal bearing strata kaolinite is decreased about 100 °C. This is explained on the basis of the interlayer space of the kaolinite increased obviously after being intercalated by KAc, which led to the interlayer hydrogen bonds weakened, enables the dehydroxylation from kaolinite surface more easily. Furthermore, the possible structural model for CSKK has been proposed, with further analysis required in order to prove the most possible structures.

Keywords Coal-bearing strata kaolinite, potassium acetate, intercalation complex, dehydroxylation, structural model

• Corresponding authors. Fax:+86 10 62331285 (Q. Liu) , +61 7 3138 2407(R. L. Frost)

E-mail addresses: lqf@cumtb.edu.cn (Q. Liu), r.frost@qut.edu.au (R. L. Frost)

1. Introduction

Kaolinite-rich mineral deposits are very abundant in the Permo-Carboniferous coal-bearing strata of North China and are widely used [1-3]. It was found that kaolinite usually existed in the upper part of sedimentary cycle, deposited vertically, which was formed in the hydrodynamic environment from strong to weak [4]. Some deposits have high carbon content and form hard minerals. The majority of coal measures in Northern China contain the industrial kaolinite rocks. Therefore, this kind of kaolinite is called as coal-bearing strata kaolinite (CSK), and the main mineral compound is kaolinite. The color of CSK is rather dark, varying from light gray to gray black to almost completely black [1, 5].

The kaolinite intercalation and its application in polymer-based functional composites have attracted great interest, both in industry and in academia fields, since they frequently exhibit remarkable improvements in materials properties compared with the virgin polymer or conventional micro and macro-composites [6-8]. The intercalation can increase the usability of kaolinite reserves especially CSK. This is due to intercalation can improve the particle size and whiteness or brightness of kaolinite. Therefore, its intercalation complexes are widely used in the fabrication of paper, paints and inks, rubber and plastic, fiberglass, cracking catalysts, cosmetics, medicines, etc [9-11]. It is useful because of their high specific surface area, chemical and physical stability, and surface structural properties [12]. Various inorganic and organic species can be used in the intercalation of kaolinite into its interlayer spaces, such as formamide [13], dimethylsulfoxide [14], urea [15], potassium acetate [16], aniline[17] and hydrazine [18]. Potassium acetate (KAc) has been shown to readily intercalate within the kaolinite structure [19, 20]. Also of significant interest regarding the kaolinite-potassium acetate complex is its thermal behavior and decomposition [19]. This is because heating treatment of intercalated kaolinite is necessary for its further application, especially in the field of plastic and rubber industry. Our recent findings showed that the onset of dehydroxylation occurs at a lower temperature than that for nonintercalated kaolinite [21-23]. Meanwhile, the more recent literature [19] also indicated that the kaolinite intercalated by KAc lead to dehydroxylation at somewhat lower temperatures than for the original kaolinite. However, to date there have been few reports regarding the temperature decrease and process interpretations of dehydroxylation for kaolinite intercalation complex.

More recently, there has been increased research on molecular simulation studies on the

intercalation of simple molecules in kaolinite [19, 24, 25]. This is because molecular simulations allow a more detailed interpretation of the experiments and might provide findings that can hardly be derived from experimental data. Although the exact structure of the kaolinite-KAc intercalation complex remains largely unknown, detailed and accurate thermal analysis can be used to furnish evidence or information on the structure of kaolinite-KAc intercalation complex. Therefore, it is very urgent and necessary for the researchers to study on the mechanism of dehydroxylation and thermal decomposition process for kaolinite intercalated by KAc.

This paper, based on authors' previous work [22, 23], reports the thermal decomposition process and dehydroxylation mechanism of coal-bearing strata kaolinite-KAc intercalation complex (CSKK) using X-ray diffraction (XRD), infrared transmission and emission spectroscopy and thermal analysis-mass spectrometric analysis. The purpose of the present study is to make clear the dehydroxylation mechanism and high temperature phase transition for CSKK or kaolinite-KAc intercalation complex and provide novel structural insight regarding the structural model of the intercalation complex.

2. Experimental

2.1. Materials

The raw materials used in this work are tonstein, which are kaolinite claystone of volcanic origin found as partings in coal seams of Permo-Carboniferous strata in Datong coal mines from Shanxi province in North China, with size of 45 μm. The beds of tonstein are ~0.5 m thick and are widespread in the coal-bearing strata of the Datong coalfield. The kaolinite content in the rocks is up to 95% with a Hinckley index of 1.10 and the quality is very good for industrial use (Table 1). Its chemical composition in wt% is SiO_2 48.69, Al_2O_3 34.34, Fe_2O_3 0.35, MgO 0.09, CaO 0.11, Na_2O 0.02, K_2O 0.38, TiO_2 0.74, P_2O_5 0.15, MnO 0.059, loss on ignition 15.07. The potassium acetate (A. R) was purchased from Beijing Chemical Reagents Company, China.

2.2. Intercalation reaction

CSKK-5, CSKK-15, CSKK-30 and CSKK-50 were prepared by immersing 10 g of CSK in 20 ml of KAc solution at concentrations of 5%, 15%, 30% and 50%, respectively. The samples were shaken for 2 h at room temperature. The intercalation complexes after aging for 24 h were allowed to dry at room temperature before the XRD, infrared transmission and emission spectroscopy and thermal

analysis-mass spectrometric analysis. Only the samples (CSK and CSKK-30) were heated in oven at 500, 600, 700, 800, 900, 1000 and 1100 °C for 4 hours before the XRD analysis.

2.3. Characterization

2.3.1. X-ray diffraction (XRD)

The XRD patterns of the prepared samples were performed using a Rigaku D/max 2500PC X-ray diffractometer with Cu (λ=1.54178 Å) irradiation at the scanning rate of 2 °/min in the 2θ range of 2.6-70 °, operating at 40 kV and 150 mA.

2.3.2. Thermal analysis-mass spectrometric analysis

The simultaneous thermogravimetry and differential scanning calorimetry (TG-DSC) measurements were carried out by a Mettler-Toledo TG-DSC I/1600 HT simultaneous thermal analyzer in a flowing nitrogen atmosphere (100 ml/min), about 30 mg of samples underwent thermal analysis with a heating rate of 5 °C/min from room temperature to 1200 °C.

The thermal analysis instrument was coupled to a Balzers (Pfeiffer) mass spectrometer (MS) for gas analysis. Only water vapour, carbon dioxide, carbon and oxygen were analysed. In the MS figures, e.g. Fig. 6, a background of broad peaks may be observed. This background occurs for all the ion current curves. The background becomes more prominent as the scale expansion is increased. It is considered that this background may be due to the loss of chemicals which have deposited in the capillary which connects the thermal analysis instrument to the MS.

2.3.3. Infrared spectroscopy (IR)

Fourier-transform infrared spectroscopy was undertaken by a Thermofisher Nicolet 6700 spectrometer. The samples were prepared at potassium bromide (KBr) pellets (ca. 2% by mass in KBr). The infrared spectra of prepared samples between 400 and 4000 cm^{-1} were recorded.

2.3.4. Infrared emission spectroscopy

Infrared emission spectroscopy was carried out on a Nicolet Nexus 870 Fourier-transform infrared spectrometer, which was modified by replacing the IR source with an emission cell. A description of the cell and principles of the emission experiment have been published elsewhere [26, 27]. Approximately 0.2 mg of CSKK was spread as a thin layer on a 6 mm diameter platinum surface and

held in an inert atmosphere within a nitrogen-purged cell during heating. The infrared emission cell consists of a modified atomic absorption graphite rod furnace, which is driven by a thyristor-controlled AC power supply capable of delivering up to 150 A at 12 V. A platinum disk acts as a hot plate to heat CSKK sample and is placed on the graphite rod. An insulated 125 -μm type R thermocouple was embedded inside the platinum plate in such a way that the thermocouple junction was less than 0.2 mm below the surface of the platinum. Temperature control of ±2 °C at the operating temperature of the sample was achieved by using a Eurotherm Model 808 proportional temperature controller, coupled to the thermocouple.

In the normal course of events, three sets of spectra are obtained over the temperature range selected and at the same temperatures; those of the black body radiation, the platinum plate radiation, and the platinum plate covered with the sample. Normally only one set of black body and platinum radiation is required. The emission spectrum at a particular temperature was calculated by subtraction of the single beam spectrum of the platinum backplate from that of the platinum covered with the sample, and the result ratioed to the single beam spectrum of an approximate black body (graphite). This spectral manipulation is carried out after all the spectral data has been collected.

The emission spectra were collected at intervals of 50 °C over the range 100-1000 °C. The time between scans (while the temperature was raised to the next hold point) was approximately 100 s. It was considered that this was sufficient time for the heating block and the powdered sample to reach temperature equilibrium. The spectra were acquired by co-addition of 128 scans for the whole temperature range, with an approximate scanning time of 1 min, and a nominal resolution of 4 cm^{-1}. Good quality spectra can be obtained providing the sample thickness is not too large. If too large a sample is used then the spectra become difficult to interpret due to the presence of combination and overtone bands. Spectral manipulation such as baseline adjustment, smoothing and normalization was performed using the Spectra calc software package (Galactic Industries Corporation, NH, USA).

3. Results and discussion

3.1. XRD results

The XRD patterns of CSK and CSKK are shown in Fig.1. The XRD pattern of CSK displays a typical and well ordered layer structure with a basal spacing (d_{001}) of 0.71 nm (Fig. 1a). This value matches well with the standard ICDD reference pattern 14-0164 (kaolinite, $Al_2Si_2O_5(OH)_4$). When CSK was intercalated with KAc, expansion occurred along the C-axis only [28]. The XRD patterns

show that the basal $d_{(001)}$ of CSK expands from 0.71 to 1.42 nm; the increment of 0.71 nm in *d*-value of CSK indicates the intercalation of KAc in the interlamellar space, which is similar to the results published before [29-31]. The effect of KAc intercalation causes the loss of the $d_{(001)}$ spacing and after the mass percentage concentration of 50% KAc intercalation the intensity significantly decreased in this peak. The significance of the loss of intensity of the $d_{(001)}$ peak means the stacking between the kaolinite layers is disrupted and lost. It is reported that an increase of the structural disorder caused an obvious weakening of reflections 11l and 02l (2θ between 17 and 27 °), which were replaced by a broad peak of scattering with weak modulations [32, 33]. This is due to the KAc intercalation has broken the hydrogen bonding between adjacent kaolinite layers. CSK intercalated with KAc causes the expansion of its layers in the c direction, and results in significant changes in its surface properties. For example, intercalation can cause significant disordering of the kaolinite, increased surface areas and provide more surface hydroxyl, which are more readily available for chemical reactions.

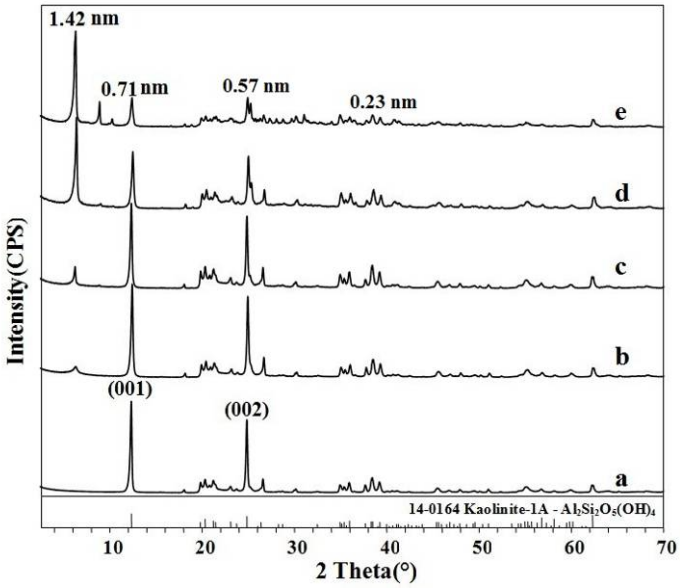

Fig.1 The XRD patterns of (a) CSK, (b) CSKK-5, (c) CSKK-15, (d) CSKK-30 and (e) CSKK-50

By using the ratio of the intensity of the *(001)* peak after and before intercalation, a measure of the degree of intercalation may be obtained [34]. For CSK intercalated by KAc with the solution concentrations of 5%, the degree of intercalation is found to be 0.12 (12% intercalated). When CSK was intercalated under the solution concentrations of 50%, the degree of intercalation is determined as 0.75 (75% intercalated).

A systematic study on the kinetics of dehydration and rehydration of the kaolinite–potassium acetate complex using XRD was made by Frost et al. [16, 35]. Upon heating the complex to 200 °C and

cooling back to room temperature in nitrogen atmosphere, two diffraction peaks appeared at 1.17 and 0.97 nm, and the 1.41 nm reflection was missing. Upon exposure to air for 1 min phases were observed with $d_{(001)}$ spacings of 1.41, 1.16, 0.99, 0.89, and 0.86 nm. The 1.41 nm phase corresponds to the fully expanded kaolinite, and the 1.16 and 0.98 nm phases correspond to the two expanded phases of the 200 °C pattern. The two expanded phases at 0.89 and 0.86 nm may correspond to the formation of a hydrated kaolinite. Although in XRD experimental examinations so far the thermal decomposition of kaolinite-KAc intercalation complex at lower temperature (<500 °C) was discussed, the thermal behavior at higher temperature is not involved. Our recent finding [22] showed that the peak intensity of the expanded phase of the kaolinite-KAc intercalation complex decreased with heating above 300 °C, and the basal spacing reduced to 1.19 nm at 350 °C and 0.715 nm at 400 °C. For further analysis of the thermal behavior for CSKK, the XRD analysis at the temperature between 500 and 1100 °C need to be considered. For convenience of discussion, the CSK intercalated by the KAc solution at concentrations of 30% was used to analyse the high temperature phase transition. Therefore, CSK and CSKK-30 were heated in oven at 500, 600, 700, 800, 900, 1000 and 1100 °C for 4 hours before the XRD analysis. Fig.2 a and b display the XRD patterns of CSK and CSKK-30 heated at 500, 600, 700, 800, 900, 1000 and 1100 °C, respectively. The XRD patterns of CSK reveal that the dehydroxylation of CSK occurred between 500 and 600 °C, and the metakaolinite was formed above 600 °C. However, there is a vast difference for the thermal behavior between CSK and CSKK-30. The intercalation complex has completed the dehydroxylation at below 500 °C. At 600 °C, the reflections of CSKK-30 and CSK disappear and new products are formed. According the standard ICDD reference pattern, it is indicated that the chemical substance $KHCO_3$ is present (marked with "*" in Fig.2 b). As the temperature of the system is raised, a small amount of K_2CO_3 is formed at 700 °C by the thermal decomposition of $KHCO_3$. At the same time, the water and carbon dioxide are released from the complex, and this will be further proved by the MS results. The formation of $KAlSiO_4$ (marked with "◆" in Fig.2 b), the structure of which is very similar to that of kaliophilite, is observed at a rather low temperature (700 °C). At 800 °C, a new compound ($K_2Al_2SiO_4$), the structure of which is the same as natrolite, is observed with the reduction by elemental carbon of K_2CO_3. At 900 °C and 1000 °C, the formation of potassium aluminum silicate ($K_4Al_2Si_2O_3$) is observed (marked with "▲" in Fig.2 b). It can be observed a considerable amount of K_3AlO_3 is formed in this intercalation complex sample until about 1100 °C. The decrease of dehydroxylation temperature and the new chemical formed may be due to

two mechanisms: 1) The potassium can decrease the melting point of chemical substance when potassium takes part in the chemical reaction with the raise of temperature; 2) The potassium ion fits into the ditrigonal holes of the oxygen-surface of CSK, and it can not be deintercalated from the interlayer. Therefore, the potassium ion exists as a chemical substance that is present at the start of a chemical reaction, resulting in the new chemical substance to appear with the raised of temperature.

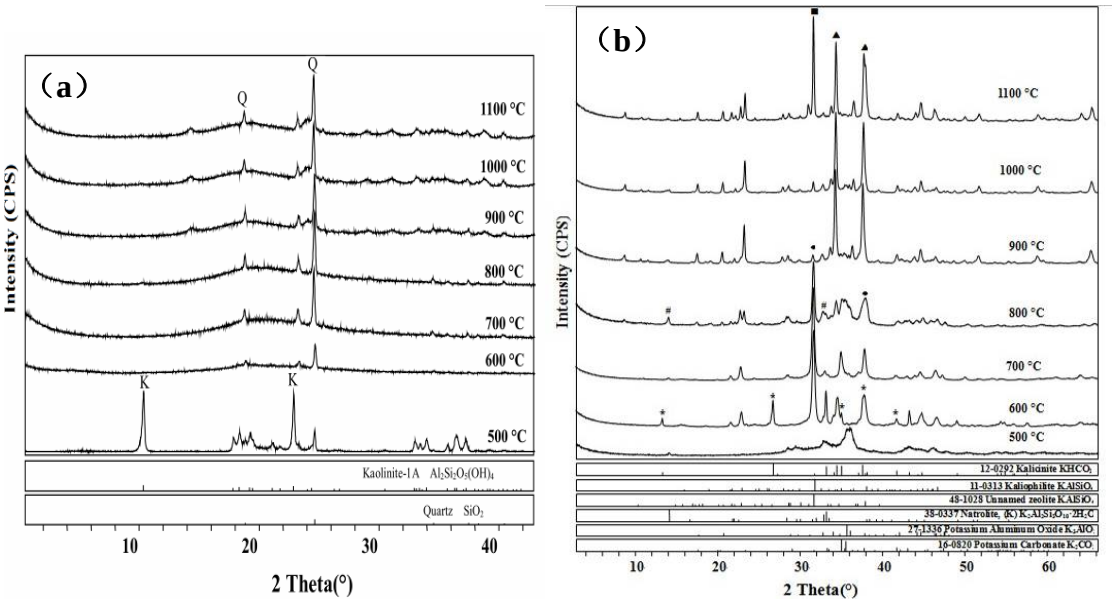

Fig.2 The XRD patterns of (a) CSK and (b) CSKK-30 heated at 500, 600, 700, 800, 900, 1000 and 1100 °C

3.2. Infrared spectroscopy

Fig.3 gives the IR spectra (4000-2500 cm^{-1} region and 2000-500 cm^{-1} region) for CSK and CSKK. The spectra of kaolinite and kaolinite-KAc intercalation complex have been described previously [16, 33, 35, 36]. As reported by Ledoux and White [36], the unit cell of kaolinite shows the existence of four hydroxyl groups. One hydroxyl group termed the inner hydroxyl, lies in the *ab* plane and points toward the apical oxygen, which is the bridging atom between the siloxane and gibbsite-like surface. The inner hydroxyls refer to the OH groups in the plane common to octahedral and tetrahedral sheets and to OH groups at 0.437 nm, both having their dipole directed towards an empty octahedral site. The other three, termed the inner surface hydroxyl group, lie at angles between 65° and 73° to the *ab* plane and point away from the surface and hydrogen bond to the oxygens of the next adjacent siloxane layer. Inner surface hydroxyls refer to OH groups located at the surface of the octahedral sheets opposite the tetrahedral oxygens of the adjacent kaolinite layer and having their OH dipole normal or nearly normal to the *(001)* plane. These hydroxyls in terms of spectroscopy function as in-phase and out-of-phase vibrations. Four distinct bands are observed in the infrared spectrum of CSK (Fig.3a). The three higher

188 frequency bands (3695, 3668 and 3650 cm^{-1}) are assigned to OH stretching modes of the three inner
189 surface hydroxyl groups. The band at 3620 cm^{-1} is attributed to the stretching of the inner hydroxyl
190 group. In the comparison of the spectra of CSK with those of CSKK, one should particularly note three
191 observations: (a) After KAc intercalation, a new (hydrogen-bonded) band appeared at 3604 cm^{-1},
192 which is due to the hydroxyl stretching vibration of the inner surface hydroxyls, which are hydrogen
193 bonded to the acetate [37]. According the report by Ledoux *et al.* [36], the formation of a hydrogen
194 bond O-H…(CH_3COO) was proposed on the basis that interaction of the acetate anion with
195 inner-surface hydroxyls had resulted in the shift of the 3695 cm^{-1} to 3604 cm^{-1}. This can be due to the
196 fact that acetate ions are situated in the interlayer position. The strong negative oxygens of the acetate
197 anions should form hydrogen bonds with inner surface hydroxyls shifting their frequencies towards
198 lower values. Furthermore, with the increase for the concentration of KAc intercalation agent, the
199 intensity of the band observed at 3604 cm^{-1} increase gradually; (b) The intensities of the bands at 3695,
200 3668 and 3650 cm^{-1} are considerably reduced whereas that of the band at 3620 cm^{-1} is not significantly
201 affected. This means that the inner hydroxyl was not affected by intercalated KAc. This result is
202 consistent with the inner hydroxyls are below the aluminium atoms and extend towards the intralayer
203 cavity (vacant octahedral site) of the kaolinite [33, 38]. Moreover, great changes in the relatively
204 intensity between the band at 3668 cm^{-1} and the band at 3650 cm^{-1} have taken place. This may be due
205 to the presence of the potassium ion affect the dipole moment of this hydroxyl group by effectively
206 “squeezing” into the ditrigonal cavity of the siloxane layer. This cavity is about 0.232 nm wide, and the
207 potassium ion is 0.233 nm in diameter; (c) The broad band below 3600 cm^{-1} is due to the hydroxyls
208 stretching frequency of interlayer water coordinated to KAc. It is reported that the kaolinite-KAc
209 intercalation complex was formed from the expansion of kaolinite with both KAc and water molecule
210 [16]. Therefore, these shift and appearance are attributed to that the water coordinated to KAc is
211 intercalated into the interlayer of kaolinite. Meanwhile, the potassium ion fits into the cavity and
212 influences both the position and the intensity of the hydroxyl vibration modes. It is pointed out that
213 KAc molecule possessing both proton-donor and proton-acceptor group is easily intercalated. The
214 acetate ion has only proton-acceptor capability and can form hydrogen bonds with the gibbsitic sheet,
215 only.

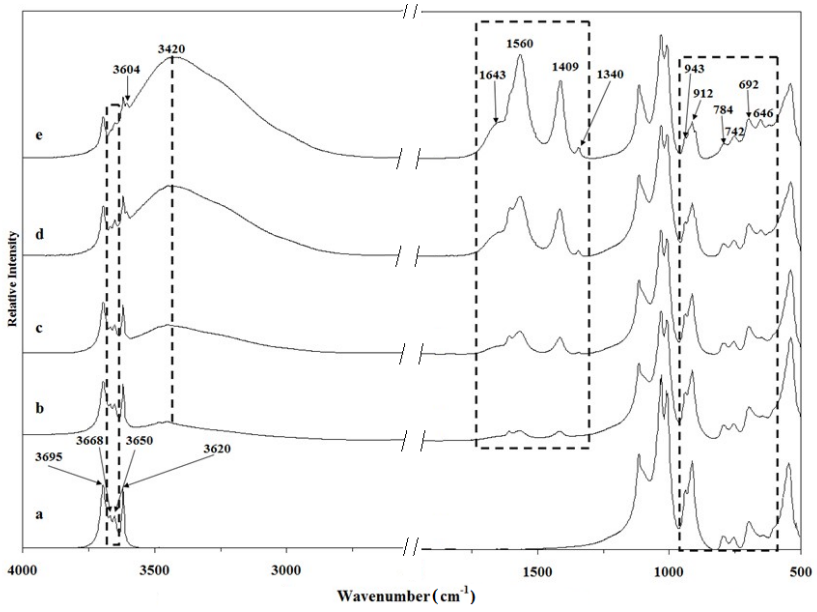

Fig.3 The infrared spectra of (a) CSK, (b) CSKK-5, (c) CSKK-15, (d) CSKK-30 and (e) CSKK-50

In the study of the intercalation of CSK with KAc, not only is it necessary to study the kaolinite hydroxyl bands but the acetate bands should also be studied. Changes in the hydroxyl-stretching bands should also be reflected in changes in the acetate bands as the acetate is hydrogen bonding to the inner surface hydroxyls. By comparing the infrared spectra of CSK and CSKK in 2000-500 cm^{-1} region, several band appearance and shift are observed. This variation of wavenumber is complex because the lattice modes and the intercalation molecule also have some influence in this region of the spectra [39]. The intercalation reaction destroys the inherent hydrogen bond of kaolinite and presents some new bonds [40]. The symmetric deformation band of the CH_3 group is observed in the spectrum at 1340 cm^{-1} for the intercalation complexes. It is proposed that this shift of CH_3 group for the acetate is due to the effect on the interlayer environment [41]. The symmetric stretching band of the O-C-O unit in KAc shifted to 1409 cm^{-1} as a result of hydrogen-bonding with inner surface OH groups in the intercalation complex. The intense band is observed at 1560 cm^{-1}, which is due to the antisymmetric ν (COO) stretching vibrations. The band is observed at 1643 cm^{-1} which appeared, but less intense, and is assigned to water bending modes within the interlayer of CSK intercalated with KAc [42]. The fact that this band is observed suggests that there is water molecule in the structure of intercalated CSK, which is different with the interlayer structure of CSK. However, it is important to note that the spectra in this region not only provide the information about the nature of the inserting molecule, but also display the characteristic bands of OH deformation. The intercalation of CSK with KAc caused significant differences in the intensities of the bands at 742 and 784 cm^{-1}, which are typical of the OH translational

vibrations. It is observed that the intensity of the OH translational vibrational bands (784 cm^{-1}) decreased when CSK intercalated with KAc. In addition, the relatively intensities of these two bands (742 and 784 cm^{-1}) changes a lot. The bands at 912 and 943 cm^{-1} are attributed to the OH bending vibrations. By contrasting CSK with CSKK, it is found that the increase in the intensity of the band at 646 cm^{-1} has coincided with the intensity drop of the band at 692 cm^{-1}. Two strong bands at 998 and 1031 cm^{-1} are assigned to the Si-O-Si in-plane vibrations. The band occurring at 1124 cm^{-1} is the Si-O stretching mode.

3.3. Thermal analysis

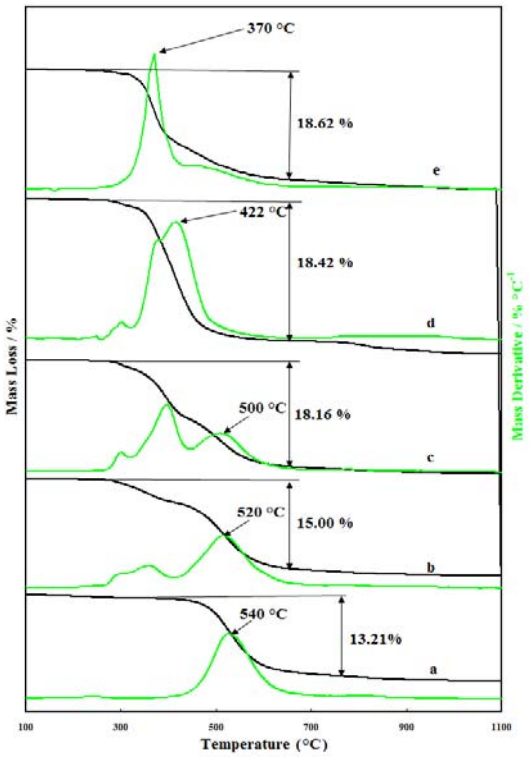

Fig.4 The TG-DTG curves for (a) CSK, (b) CSKK-5, (c) CSKK-15, (d) CSKK-30 and (e) CSKK-50

The thermogravimetric and differential thermogravimetric (TG-DTG) measurement of CSK and CSKK are performed and results are shown in Fig. 4. Only one mass loss is observed in the TG-DTG curves of CSK in Fig.4a at 540 °C with mass loss of 13.21 %, which is attributed to the dehydroxylation of kaolinite. This value was close to the theoretical value (13.9 %). However, various mass losses are observed in the TG curves of CSKK in Fig. 4b, c, d, e. The DTG curve of the intercalation complex (Fig.4b) presented a broad peak at 520 °C associated with dehydroxylation of the intercalated CSK with a 15.0 % mass loss. The fourth TG-DTG curves for CSKK-30 (Fig.4d) presented a mass loss of 18.42 % between 300 and 500 °C with a maximum rate at 422 °C is attributed to a set of

steps for the dehydration, loss of KAc and dehydroxylation of the intercalation complex at the elevated temperature. It is well known that CSKK was formed from the expansion of CSK with both KAc and water molecule [35, 43]. Therefore, this step can be interpreted as being due to the loss of intercalated water which is coordinated to KAc in the interlayer of CSK. These results agree with our previous studies [22, 44], where an increase in the rate of mass loss at 370 °C for the intercalation sample corresponded to dehydroxylation of CSKK-50 along with the liberation of a small amount of acetate decomposition products.

It would be easy to come to this conclusion that the temperature of dehydroxylation for CSK intercalated by KAc and the concentration of KAc intercalation agent are negative linearity correlativity. With the increase for the concentration of KAc intercalation agent, the temperature of dehydroxylation for CSKK sharply decreases from 540 °C to 370 °C. This is may be due to two mechanisms:

1) After intercalated by KAc, the interlayer distance of kaolinite is expanded, thus the interlayer hydrogen bonds weakened, results in the dehydroxylation from kaolinite surface more easily. In addition, the crystallinity of kaolinite after intercalation decreases sharply. It was reported that the temperature of dehydroxylation depending on the crystallinity is typical for most kaolinites [45].

2) The dehydroxylation process of kaolinite can be influenced by the pressure of water vapour. When the system was hot and interlayer water was being heated, the water vapour was rising in the layer of intercalated kaolinite.

Fig. 5a displays the DSC curve of CSK and clearly shows an endothermic peak at 540 °C corresponding to its dehydroxylation in addition to an exothermic peak at 998 °C associated with the formation of a spinel phase that was transformed into mullite [46, 47]. However, there are two endothermic peaks at 285 and 520 °C for the intercalation complex in Fig.5b. It is therefore concluded that the endothermic peak at 285 °C is due to the loss the intercalated water, the endothermic peak at 520 °C results from the dehydroxylation of the intercalated CSK. This will be further proved by the mass spectrometric analysis and infrared emission spectroscopic analysis.

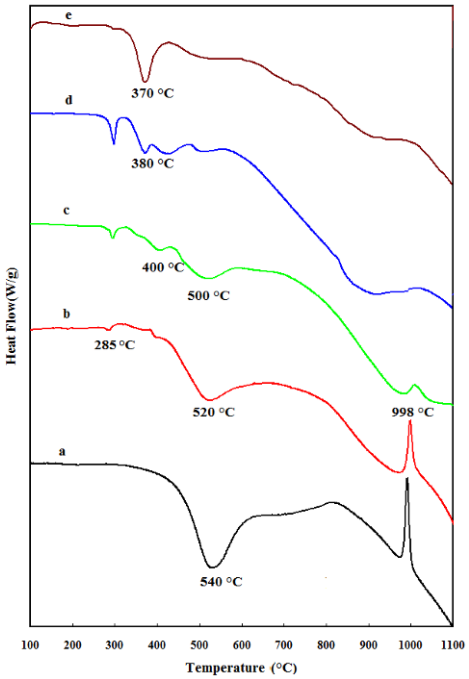

Fig.5 The DSC curves of (a) CSK, (b) CSKK-5, (c) CSKK-15, (d) CSKK-30 and (e) CSKK-50

The maximum rate of mass loss for CSKK-50 is observed at 370 °C, instead of 540 °C, for CSK sample. The temperature of dehydroxylation for CSK intercalated by KAc decreased significantly. The DSC curve at 998 °C indicates no spinel phase that was transformed into mullite of the intercalated sample. It is possible that the obtained solid potassium compound prohibits the formation of a crystalline spinel phase [48, 49]. It can be seen from the XRD that during the heat treatment of CSKK potassium aluminum silicates formed. These phases can form thermodynamically at the given chemical composition. Therefore, the thermal analysis results are correspondent with the XRD results.

3.4. Mass spectrometric analysis

To better understand the thermal decomposition and dehydroxylation mechanisms of kaolinite intercalation complex, the CSK intercalated by KAc with the solution concentrations of 30%, which has high degree of intercalation and the regent KAc is not excessive for intercalation, were selected to analyse the thermal decomposition products for the intercalation complex. In accordance with former findings several different steps of dehydration have occurred. In order to clarify the thermal decomposition mechanism of CSKK and understand well the dehydration of interlayer and structural water for this complex, the mass loss during each decomposition process should be characterized by the identified evolution components. The mass spectrometric data also provide evidence on the thermal decomposition products.

The interpretation of the mass spectra occurs on the basis of degassing profiles from the molecule ions of water (H_2O^+: m/Z=18), carbon dioxide (CO_2^+: m/Z=44) as well as by fragment ions (OH^+: m/Z=17, O^+: m/Z=16).

The evolution of gas species has been followed *in situ* by the coupled TG-MS system. The evolution curves of ion-fragments of various gases released are shown as ion current versus temperature curves in Fig. 6. The characterization of water release by means of mass spectra is possible with the molecule ion H_2O^+ (m/Z=18) together with the fragment ion OH^+ (m/Z=17) and O^+ (m/Z=16). Peaks at 285 and 422 °C for the intercalation complex are found in the ion current curve for H_2O^+ (m/Z=18); corresponding peaks are also found in the ion current curves for OH^+ (m/Z=17) and O^+ (m/Z=16). It can be safely concluded that the water is given out at about 285 °C and at 422 °C for CSKK. Moreover, the broad peak at 407 °C is found in the ion current curve for CO_2^+ (m/Z=44). This illustrate a small proportion of CO_2 is given out in this temperature range. Another broad peak in the ion current curve for CO_2^+ (m/Z=44) is observed between 600 and 900 °C with the maximum rate at 735 °C, which is attributed to thermal decomposition of $KHCO_3$ and K_2CO_3.

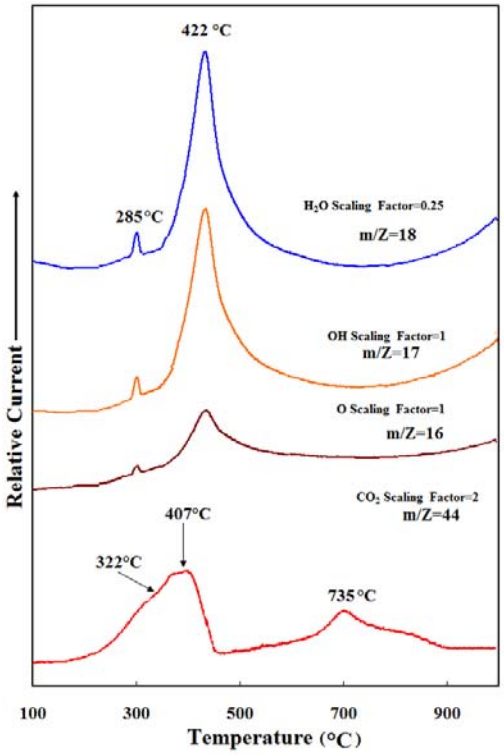

Fig.6 Evolved gas analysis for CSKK-30

According to experimental results of thermal analysis and the mass spectrometric analysis, the mass losses at 285 and 422 °C for the complex is attributed to the loss of water, and the mass loss

between 300 and 420 °C for the complex is assigned to decomposition of acetate and the dehydroxylation of the intercalated CSK. The carbon dioxide released from the complex is observed between 600 and 900 °C, which is due to the thermal decomposition of $KHCO_3$ and K_2CO_3. This result is in good agreement with XRD and thermal analysis. In addition, according the report by Makó *et al.* [24], the thermal decomposition of kaolinite-KAc complex is divided into two steps: the first step at 376 °C and, then, a slow process over a wide temperature range between 400 and 550 °C. It was also stated that early dehydroxylation is due to the removal of inner surface hydroxyls which are hydrogen bonded to the intercalating acetate ions, while the second step is due to the removal of hydroxyls which are not hydrogen-bonded to the acetate. Therefore, it is concluded that the water associated with acetate and Al^{3+}-OH was removed at 285 °C and then the acetate between the layers of kaolinite was decomposed. The mass loss close to 400 °C was interpreted as decarboxylation of acetate [47].

3.5. Infrared emission spectroscopy

In order to confirm the results obtained from thermal analysis and understand the thermal decomposition of intercalation complex better, infrared emission spectroscopy was undertaken. Thermal analysis and mass spectrometric analysis clearly show at which temperature the mass loss. However, infrared emission spectroscopy will give the evidence on the changes of structure. These make all explanation have the sufficient evidence. Fig. 7 shows the infrared emission spectra of CSKK-30. The spectra clearly show the temperature at which the OH group is lost and at which the complex decomposed. For convenience of discussion, the spectra for CSKK-30 (Fig.7) are divided into two sections; they are (a) the 4000-3000 cm^{-1} region attributed to the hydroxyl stretching vibration; (b) the 1850-650 cm^{-1} region attributed to the inserting molecular vibration, the OH translational vibration and the aluminosilicate framework.

Fig. 7 illustrates the infrared emission spectra in 4000-3000 cm^{-1} region of the hydroxyl stretching bands of CSKK-30 over the temperature range 100 to 1000 °C. The figure clearly shows the loss of intensity of these bands as the temperature is raised. The following conclusions are drawn from these analyses. First, the inner surface hydroxyls are lost before the inner hydroxyls. Second, the intensity of the band for the inner surface hydroxyls hydrogen bonded to the acetate ion decreased with decreasing the intensity of the band for the hydroxyls stretching of interlayer water coordinated to KAc when the temperature is higher than 250 °C. Therefore, it can be concluded that the intercalated water was lost in the temperature range of 250 to 300 °C, and then the intensity of the hydroxyl stretching vibration of

the inner surface hydroxyl hydrogen bonded to the acetate is decreased, followed by the loss of the inner surface hydroxyl at 350 °C, and finally the inner hydroxyl is lost at 500 °C.

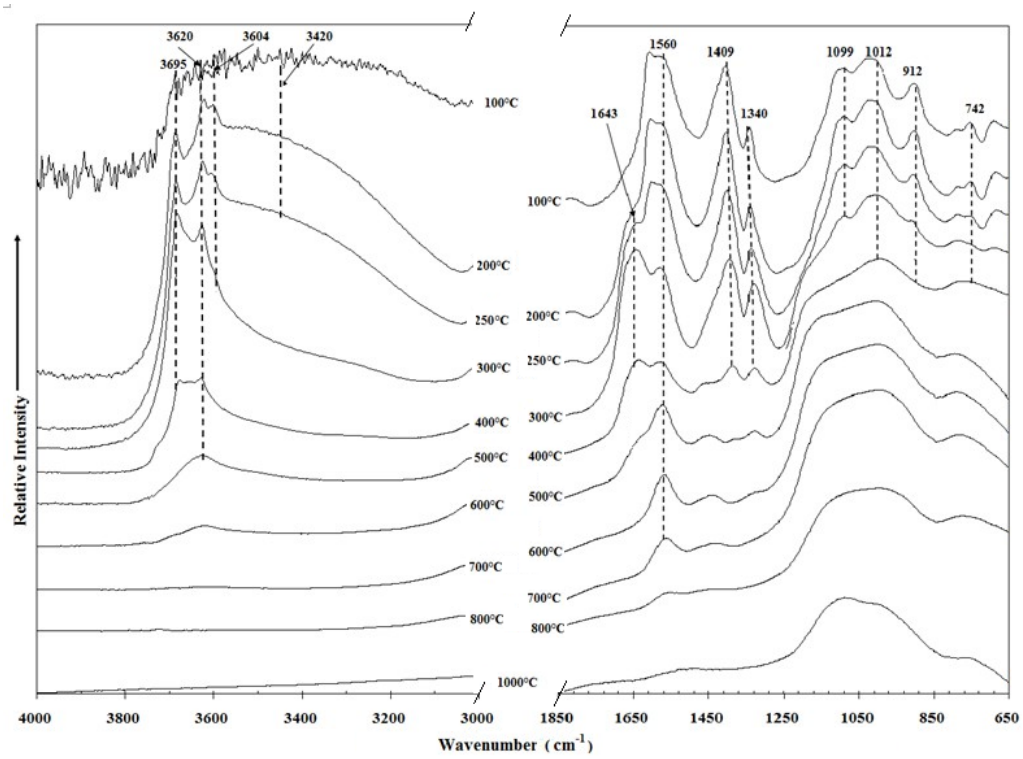

Fig.7 Infrared emission spectra of CSKK-30 over the 100-1000 °C

The infrared emission spectra of CSKK-30 in the 1850-650 cm^{-1} over the temperature range 100 to 1000 °C are shown in Fig. 7. The intensity of the CH_3 symmetric deformation vibration and the O-C-O symmetric stretching vibration in KAc is lost at 350 °C. The band at 1643 cm^{-1} is not observed at 400 °C or above this temperature. Therefore, the intercalated water is lost below 400 °C, which is consistent with the thermal analysis data and the result before [22]. The antisymmetric ν (COO) stretching vibrations observed at 1560 cm^{-1} is lost at 850 °C. This may prove once again that the $KHCO_3$ and K_2CO_3 are present in the process of thermal decomposition of the intercalation complex. Two bands at 742 and 912 cm^{-1} disappeared and a new band is observed at 784 cm^{-1} for CSKK-30. These shift and disappearance are attributed to that the water coordinated to acetate is lost when the temperature is raised. These also illustrate that when KAc is actually intercalated into the layer of kaolinite and attached with the inner surface hydroxyl of kaolinite it will result in the shift of AlO-H.

Again carefully analyse the infrared emission spectroscopic results for CSKK-30 one time, it can be seen that there is a sequence of the dehydroxylation in the intercalation complex, with the hydrogen-bonded OH groups of kaolinite disappearing first (by 300 °C), followed by all the outer

hydroxyls by 350 °C [48]. Dehydroxylation of CSKK-30 is completed at below 500 °C, and the $KHCO_3$ and K_2CO_3 are present in the process of thermal decomposition of CSKK-30. The thermal decomposition of $KHCO_3$ and K_2CO_3 is completed at 850 °C.

4. Decomposition for kaolinite intercalated by potassium acetate

The decomposition of the kaolinite-KAc intercalation complex must be interpreted on the basis of the structural arrangement of the KAc and associated water between the kaolinite layers. However, as previous reported vary widely, no unanimous conclusion can be drawn. The paper of Wada [43] was the first investigation to suggest detailed atomistic models for the kaolinite-KAc intercalation complex. This model showed that potassium occupied the ditrigonal holes of the oxygen-surface of kaolinite whereas water formed a layer between the acetate ions and the inner surface OH groups of the kaolinite. On the contrary, it was reported by Kristóf *et al.* [50] that potassium is hydrated and so departed from the acetate ions. This is in striking contrast with the structural model proposed by Wada. Nevertheless these authors did point out that water has an important role in the structure of the intercalation complex. Following this interpretation, our previous finding showed that water molecules fill the space between the expanded kaolinite layers and form primary and secondary spheres of hydration. This interpretation is based on the detailed study of the behavior of the IR bands at ~1630 cm^{-1}, ascribed to the water H-O-H bending. Conversely, Cruz and Duro [51] reported that water is present even in the `dehydrated' complex, thus suggesting the presence of H-bonds between kaolinite and water, as proposed by Wada, [43] which may persist after the partial dehydration of the complex. It also proposed by Smith *et al.* [52] that the lone pair electrons of the carbonyl oxygen in the acetate ion are more available for hydrogen bonding than those of the siloxane groups of kaolinite. Thus, as the water content in the kaolinite-KAc-water system decreases, the carbonyl oxygen of the acetate ion interacts with a hydroxyl group of kaolinite to give a stronger hydrogen bond than had existed between Si-O and Al-OH group, and intercalation begins. On the other hand, a structural arrangement with potassium occupying the ditrigonal holes of the oxygen surface of kaolinite would favor the electrostatic interactions between the keyed potassium ions and the oxygen of the inner OH groups, which justifies the modifications of the 3620 cm^{-1} hydroxyls stretching band. A structural configuration on this intercalation complex has been reported by Makó *et al.* [24], which corresponded to the 1.4 nm spacing consisted of a double layer of KAc(anhydrous). Furthermore, this phase was proposed to be anhydrous, contrary to previous

investigations on this intercalation complex. It was reported by White *et al.* [19] that this structural configuration proposed by Makó et al. was implausible due to the lack of water, which made this model inconsistent with the thermal analysis results.

If the kaolinite is intercalated with a salt of a short-chain aliphatic acid such as potassium acetate, then a concomitant decrease in the intensity of some hydroxyl bands is observed. This result is in good agreement with the result of infrared spectroscopy. From the results presented in this investigation, and the available evidence pointing towards the inclusion of potassium within kaolinite-KAc intercalation complex [19, 22, 23, 43, 53, 54], we concluded that the most possible structural model and thermal decomposition processes for the kaolinite-KAc intercalation complex is shown in Fig. 8.

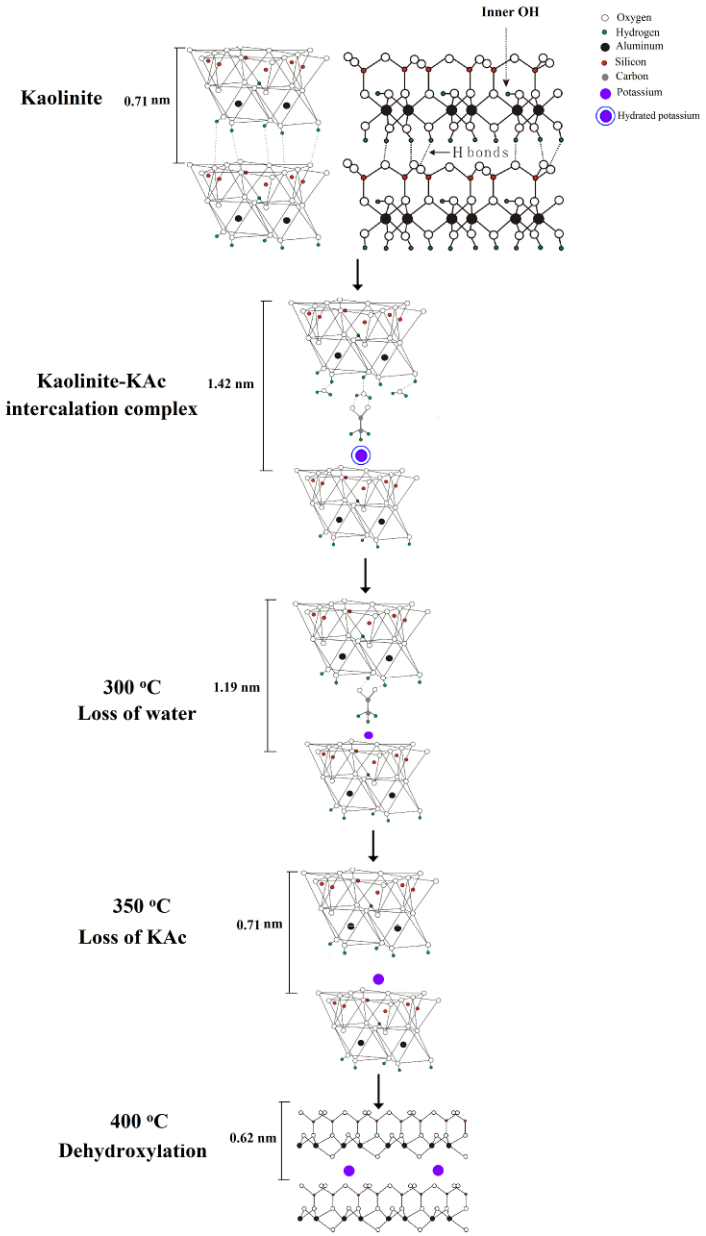

Fig.8 The most possible structural model and thermal decomposition processes for kaolinite-KAc intercalation complexes

406 The kaolinite-KAc intercalation complex is formed from the expansion of kaolinite with both KAc
407 and molecular water. It is pointed out that KAc molecule possessing both proton-donor and
408 proton-acceptor group is easily intercalated. The acetate ion has only proton-acceptor capability and
409 can form hydrogen bonds with the gibbsitic sheet through the lone pair of electrons on the C=O group.
410 Meanwhile, the potassium ion fits into the ditrigonal cavity and influences both the position and the
411 intensity of the hydroxyl vibration modes. The presence of the potassium ion may affect the dipole
412 moment of this hydroxyl group by effectively “squeezing” into the ditrigonal cavity of the siloxane
413 layer. This cavity is about 0.232 nm wide, and the potassium ion is 0.233 nm in diameter. The effect of
414 increase temperature may allow this potassium to fit into this ditrigonal or at least sit above the cavity.
415 It is therefore proposed that the thermal decomposition processes for kaolinite-KAc intercalation
416 complexes is presented as mentioned above (Fig.8). The first step is loss of the water coordinated to
417 KAc in the intercalated kaolinite. And then the inner surface hydroxyls and hydrogen bonds formed
418 water and loss resulting in the incomplete collapse of the expanded kaolinite structure to 1.1 nm. The
419 third step is attributed to the loss of the acetate in the layer of kaolinite. The last step is to loss of the
420 inner hydroxyls.

421 ## 5. Conclusions

422 The thermal decomposition processes, and the possible structure models for CSKK, have been
423 studied using TG-DSC, infrared emission spectroscopy. The kaolinite intercalated with KAc causes the
424 expansion of its layers in the *c* direction, and results in significant weaken the interlayer hydrogen
425 bonds. A comparison of thermal analysis results of CSK and CSKK gives new discovery that not only a
426 new mass loss peak is observed at 285 °C, but also the temperature of dehydroxylation and dehydration
427 of kaolinite is decreased about 100 °C. This is explained on the basis of the interlayer space of the
428 kaolinite increased obviously after being intercalated by KAc, which led to the interlayer hydrogen
429 bonds weakened, enables the dehydroxylation from kaolinite surface more easily. The DSC curve at
430 998 °C indicates no spinel phase that was transformed into mullite of the intercalated sample, and the
431 XRD results show that during the heat treatment of CSKK potassium aluminum silicates formed. These
432 phases can form thermodynamically at the given chemical composition. Upon heating, the intercalation
433 complex transitions to an amorphous state at a lower temperature than the nonintercalated kaolinite
434 counterpart, as shown through analysis of changes to the local structural correlations with temperature.

435 The most possible structural models of the kaolinite-KAc intercalation complex have been
436 proposed. According to the results presented in this investigation, and the available evidence pointing
437 towards the inclusion of potassium within the kaolinite-KAc intercalation complex, it is proposed that
438 potassium is hydrated and so departed from the acetate ions, and has been tentatively assigned to
439 occupy the ditrigonal holes of the oxygen-surface of kaolinite. The presence of the potassium ion may
440 affect the dipole moment of this hydroxyl group by effectively “squeezing” into the ditrigonal cavity of
441 the siloxane layer. The effect of increase temperature may allow this potassium to fit into this ditrigonal.
442 Furthermore, the carbonyl oxygen of the acetate ion interacts with a hydroxyl group of kaolinite to give
443 a stronger hydrogen bond than had existed between Si-O and Al-OH group.

444

445 ## Acknowledgements

446 The authors gratefully acknowledge the financial support provided by the National Natural Science
447 Foundation of China (51034006) and China Postdoctoral Science Foundation funded project (2011M500034).
448 The infra-structure support of the Queensland University of Technology, Chemistry Discipline, Faculty of
449 Science and Technology is thanked.

References

[1] Q. Liu, D.A. Spears, Q. Liu, Appl. Clay. Sci. 19 (2001) 89.

[2] H. Cheng, Q. Liu, J. Yang, R.L. Frost, Thermochim. Acta 507-508 (2010) 84.

[3] H. Cheng, J. Yang, Q. Liu, J. Zhang, R.L. Frost, Spectrochim. Acta A 77 (2010) 856.

[4] S.L. Ding, Q.F. Liu, Y.Z. Sun, B.H. Xu, World Journal of Engineering 6 (2009) 1.

[5] S.L. Ding, Q.F. Liu, M.Z. Wang, Procedia Earth Planetary Sci. 1 (2009) 1024.

[6] R.L. Frost, E. Horváth, É. Makó, J. Kristóf, J. Colloid Interface Sci. 270 (2004) 337.

[7] J.E.F.C. Gardolinski, G. Lagaly, Clay. Miner. 40 (2005) 547.

[8] X. Jia, Y. Li, B. Zhang, Q. Cheng, S. Zhang, Mater. Res. Bull. 43 (2008) 611.

[9] F. Franco, L.A. Pérez-Maqueda, J.L. Pérez-Rodríguez, J. Colloid Interface Sci. 274 (2004) 107.

[10] F. Franco, J.A. Cecila, L.A. Pérez-Maqueda, J.L. Pérez-Rodríguez, C.S.F. Gomes, Appl. Clay. Sci. 35 (2007) 119.

[11] H. Cheng, Q. Liu, J. Zhang, J. Yang, R.L. Frost, J. Colloid Interface Sci. 348 (2010) 355.

[12] H. Liu, D. Yang, E. R.Waclawik, X. Ke, Z. Zheng, H. Zhu, R.L. Frost, J. Raman Spectrosc. 41(2010) 1792.

[13] E. Joussein, S. Petit, B. Delvaux, Appl. Clay. Sci. 35 (2007) 17.

[14] P.M. Costanzo, J. R. F. Giese, Clays Clay Miner. 34 (1986) 105.

[15] K.P. Nicolini, C.R.B. Fukamachi, F. Wypych, A.S. Mangrich, J. Colloid Interface Sci. 338 (2009) 474.

[16] R.L. Frost, J. Kristof, E. Horvath, J.T. Kloprogge, J. Colloid Interface Sci. 226 (2000) 318.

[17] V. Luca, S. Thomson, J Mater Chem 10 (2000) 2121.

[18] E. Horváth, J. Kristóf, R. Frost, Á. Rédey, V. Vágvölgyi, T. Cseh, J. Therm. Anal. Calorim. 71 (2003) 707.

[19] C.E. White, J.L. Provis, L.E. Gordon, D.P. Riley, T. Proffen, J.S.J. van Deventer, Chem. Mater. 23 (2010) 188.

[20] H. Cheng, Q. Liu, J. Yang, X. Du, R.L. Frost, Appl. Clay. Sci. 50 (2010) 476.

[21] H. Cheng, Q. Liu, J. Yang, J. Zhang, R.L. Frost, Thermochim. Acta 511 (2010) 124.

[22] H. Cheng, Q. Liu, J. Yang, Q. Zhang, R.L. Frost, Thermochim. Acta 503-504 (2010) 16.

[23] H. Cheng, J. Yang, R. Frost, Q. Liu, Z. Zhang, J. Therm. Anal. Calorim. 103 (2011) 507.

[24] É. Makó, G. Rutkai, T. Kristóf, J. Colloid Interface Sci. 349 (2010) 442.

[25] G. Rutkai, É. Makó, T. Kristóf, J. Colloid Interface Sci. 334 (2009) 65.

[26] R.L. Frost, S. Bahfenne, J. Graham, Spectrochim. Acta A 71 (2008) 1610.

[27] R. Frost, D. Wain, J. Therm. Anal. Calorim. 91 (2008) 267.

[28] B. Zhang, Y. Li, X. Pan, X. Jia, X. Wang, J. Phys. Chem. Solids 68 (2007) 135.

[29] F. Franco, M.D. Ruiz Cruz, Clay. Miner. 39 (2004) 193.

[30] Y. Deng, G.N. White, J.B. Dixon, J. Colloid Interface Sci. 250 (2002) 379.

[31] R.L. Frost, J. Kristof, G.N. Paroz, J.T. Kloprogge, J. Colloid Interface Sci. 208 (1998) 216.

[32] D.N. Hinckley, Clay. Clay. Miner. 11 (1963) 229.

[33] R.L. Frost, J. Kristof, T.H. Tran, Clay. Miner. 33 (1998) 605.

[34] A. Wiewióra, G.W. Brindley, in: L. Heller, Proceedings of the International Clay Conference Israel University Press, Jerusalem, Tokyo, 1969, p 723.

[35] R.L. Frost, J. Kristof, J.T. Kloprogge, E. Horvath, Langmuir 16 (2000) 5402.

[36] R.L. Ledoux, J.L. White, Science 143 (1964) 244.

[37] R.L. Frost, J. Kristof, J.T. Kloprogge, E. Horvath, J. Colloid Interface Sci. 246 (2002) 164.
[38] J. Kristof, R.L. Frost, A. Felinger, J. Mink, J. Mol. Struct. 410-411 (1997) 119.
[39] M. Suarez, E. Garcia-Romero, Appl. Clay Sci. 31 (2006) 154.
[40] S. Mellouk, S. Cherifi, M. Sassi, K. Marouf-Khelifa, A. Bengueddach, J. Schott, A. Khelifa, Appl. Clay Sci. 44 (2009) 230.
[41] E. Horváth, J. Kristóf, R.L. Frost, Appl. Spectrosc. Rev. 45 (2010) 130.
[42] R. Liu, R.L. Frost, W.N. Martens, Mater. Chem. Phys. 113 (2009) 707.
[43] K. Wada, Am. Mineral. 46 (1961) 78.
[44] R.L. Frost, J. Kristof, E. Mako, J.T. Kloprogge, Langmuir 16 (2000) 7421.
[45] A. Shvarzman, K. Kovler, G.S. Grader, G.E. Shter, Cement Concrete Res. 33 (2003) 405.
[46] M.D.R. Cruz, F. Franco, Clay. Clay. Miner. 48 (2000) 586.
[47] K. Orzechowski, T. Slonka, J. Glowinski, J. Phys. Chem. Solids 67 (2006) 915.
[48] M. Gabor, M. Toth, J. Kristof, G. Komaromi-Hiller, Clay. Clay. Miner. 43 (1995) 223.
[49] J. Li, H. Lin, J. Li, J. Wu, J. Eur. Ceram. Soc. 29 (2009) 2929.
[50] J. Kristóf, J. Mink, E. Horváth, M. Gábor, Vib. Spectrosc. 5 (1993) 61.
[51] M.D. Ruiz Cruz, F.I.F. Duro, Clay. Miner. 34 (1999) 565.
[52] D.L. Smith, M.H. Milford, J.J. Zuckerman, Science 153 (1966) 741.
[53] H. Cheng, Q. Liu, J. Yang, J. Zhang, R.L. Frost, X. Du, J. Mol. Struct. 990 (2011) 21.
[54] J. Zhang, H. Cheng, Q. Liu, J. He, R.L. Frost, J. Mol. Struct. 994 (2011) 55.

LIST OF TABLE

Table 1 The minerals composition of CSK used in this experiment

Table 1 The minerals composition of CSK used in this experiment

Sample	**Content of minerals (%)**		
	kaolinite	Quartz	Illite
Coal bearing strata kaolinite	95	3	2

LIST OF FIGURES

Fig.1 The XRD patterns of (a) CSK, (b) CSKK-5, (c) CSKK-15, (d) CSKK-30 and (e) CSKK-50

Fig.2 The XRD patterns of (a) CSK and (b) CSKK-30 heated at 500, 600, 700, 800, 900, 1000 and 1100 °C

Fig.3 The infrared spectra of (a) CSK, (b) CSKK-5, (c) CSKK-15, (d) CSKK-30 and (e) CSKK-50

Fig.4 the TG-DTG curves for (a) CSK, (b) CSKK-5, (c) CSKK-15, (d) CSKK-30 and (e) CSKK-50

Fig.5 the DSC curves of (a) CSK, (b) CSKK-5, (c) CSKK-15, (d) CSKK-30 and (e) CSKK-50

Fig.6 Evolved gas analysis for CSKK-30

Fig.7 Infrared emission spectra of CSKK-30 over the 100-1000 °C

Fig.8 The most possible structural model and thermal decomposition processes for kaolinite-KAc intercalation complexes

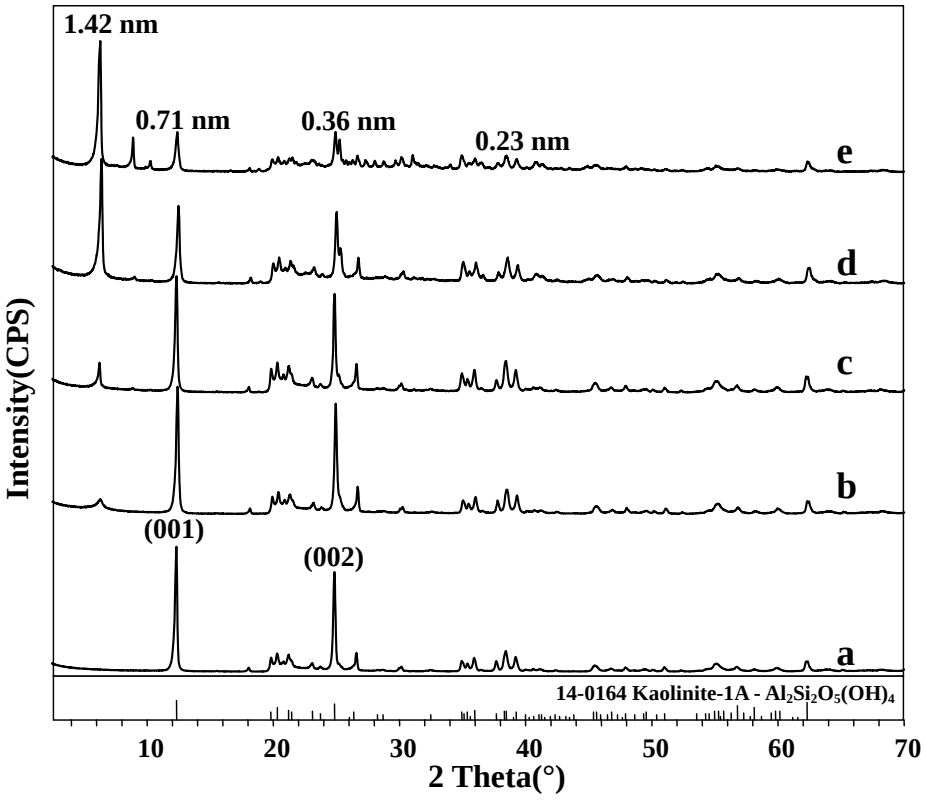
1.42 nm
0.71 nm
0.36 nm
0.23 nm
e
d
c
b
(001)
(002)
a
14-0164 Kaolinite-1A - Al2Si2O5(OH)4
Intensity(CPS)
10
20
30
40
50
60
70
2 Theta(°)

Fig.1

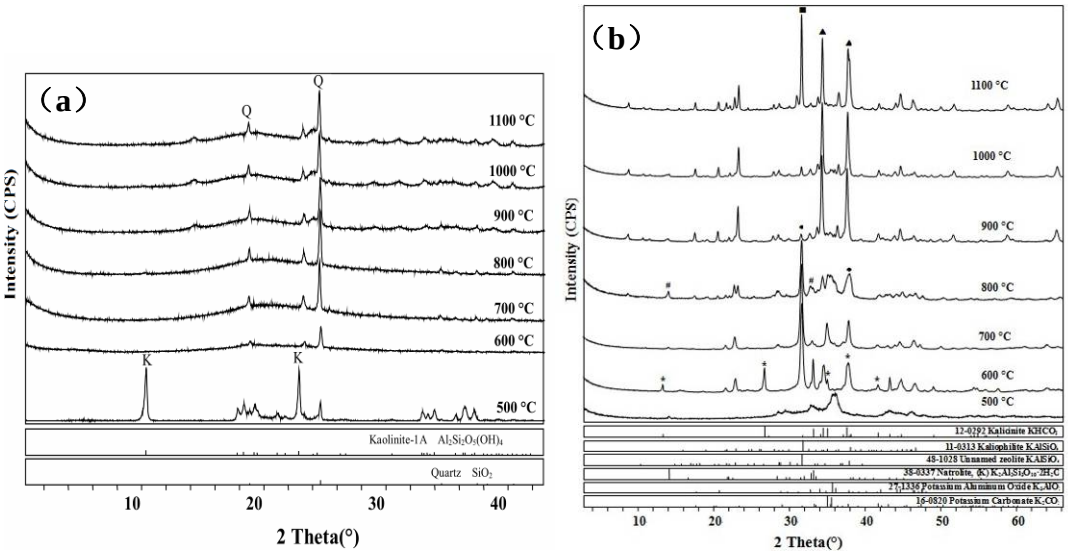
(a)
Q
Q
1100 °C
1000 °C
900 °C
800 °C
700 °C
600 °C
K
K
500 °C
Kaolinite-1A Al2Si2O5(OH)4
Quartz SiO2
Intensity (CPS)
10
20
30
40
2 Theta(°)
(b)
1100 °C
1000 °C
900 °C
800 °C
700 °C
600 °C
500 °C
12-0792 Kalicinite KHCO3
11-0313 Kaliophilite KAlSiO4
48-1028 Unnamed zeolite KAlSiO4
38-0337 Natrolite, (K) K2Al2Si3O10·2H2O
27-1336 Potassium Aluminum Oxide K2AlO2
16-0820 Potassium Carbonate K2CO3
Intensity (CPS)
10
20
30
40
50
60
2 Theta(°)

Fig.2

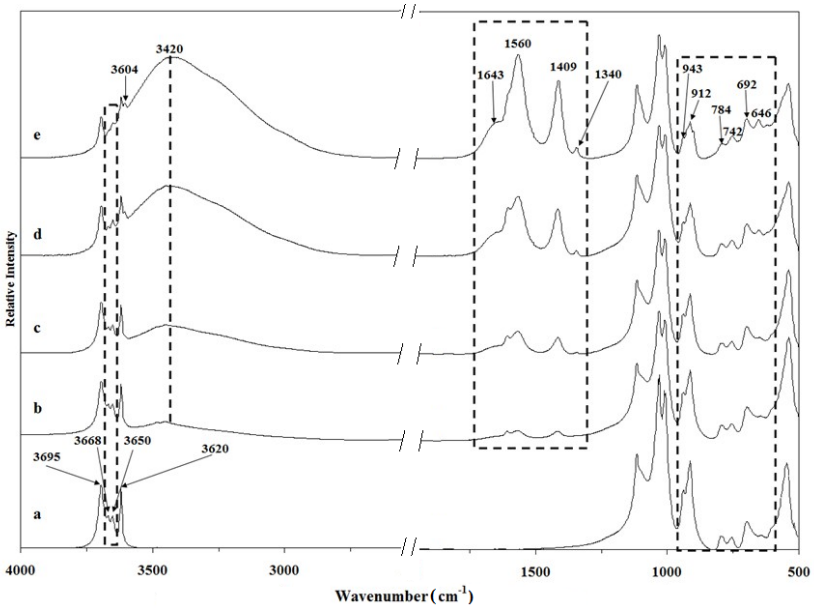
3420
3604
1560
1643
1409
1340
943
912
784
742
692
646
e
d
c
b
a
3695
3668
3650
3620
Relative Intensity
4000
3500
3000
1500
1000
500
Wavenumber(cm-1)

Fig.3

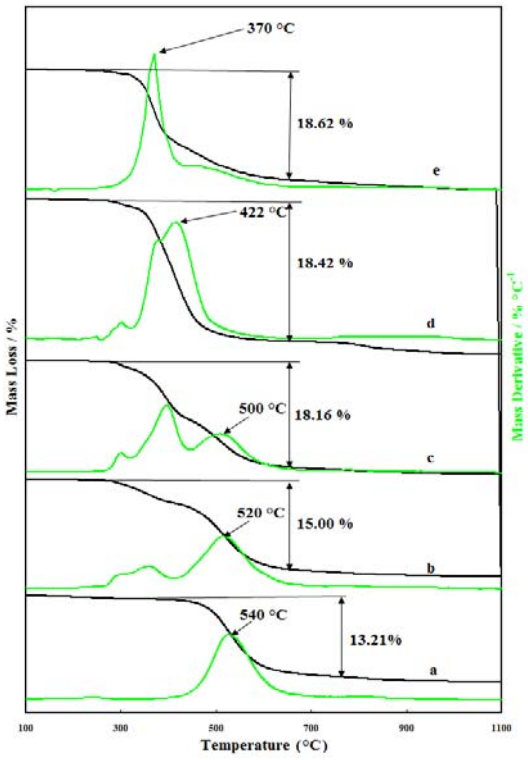
370 °C
18.62 %
e
422 °C
18.42 %
d
500 °C
18.16 %
c
520 °C
15.00 %
b
540 °C
13.21%
a
Mass Loss / %
Mass Derivative / % °C⁻¹
100
300
500
700
900
1100
Temperature (°C)

Fig.4

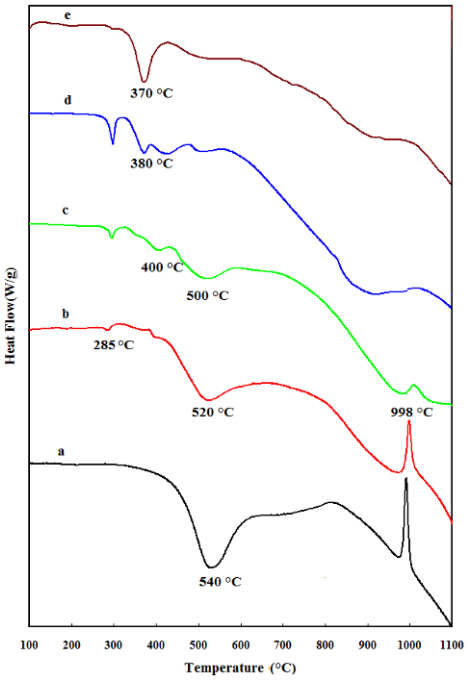
e
370 °C
d
380 °C
c
400 °C
500 °C
b
285 °C
520 °C
998 °C
a
540 °C
Heat Flow(W/g)
100 200 300 400 500 600 700 800 900 1000 1100
Temperature (°C)

Fig.5

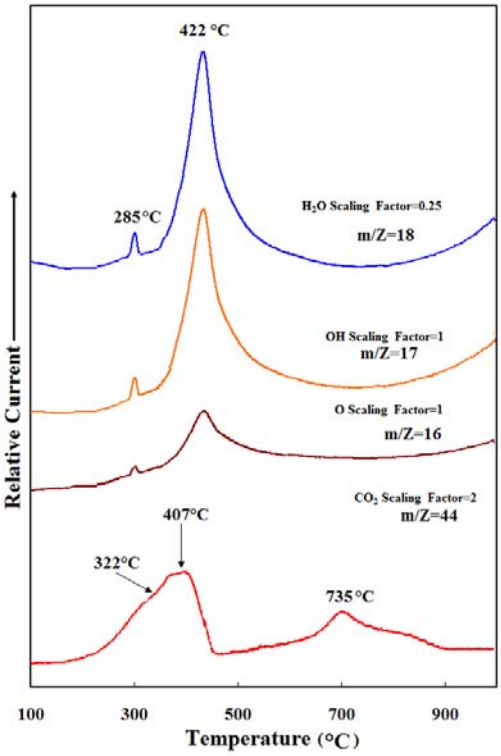
422 °C
285°C
H2O Scaling Factor=0.25
m/Z=18
OH Scaling Factor=1
m/Z=17
O Scaling Factor=1
m/Z=16
CO2 Scaling Factor=2
m/Z=44
407°C
322°C
735°C
Relative Current
100
300
500
700
900
Temperature (°C)

Fig.6

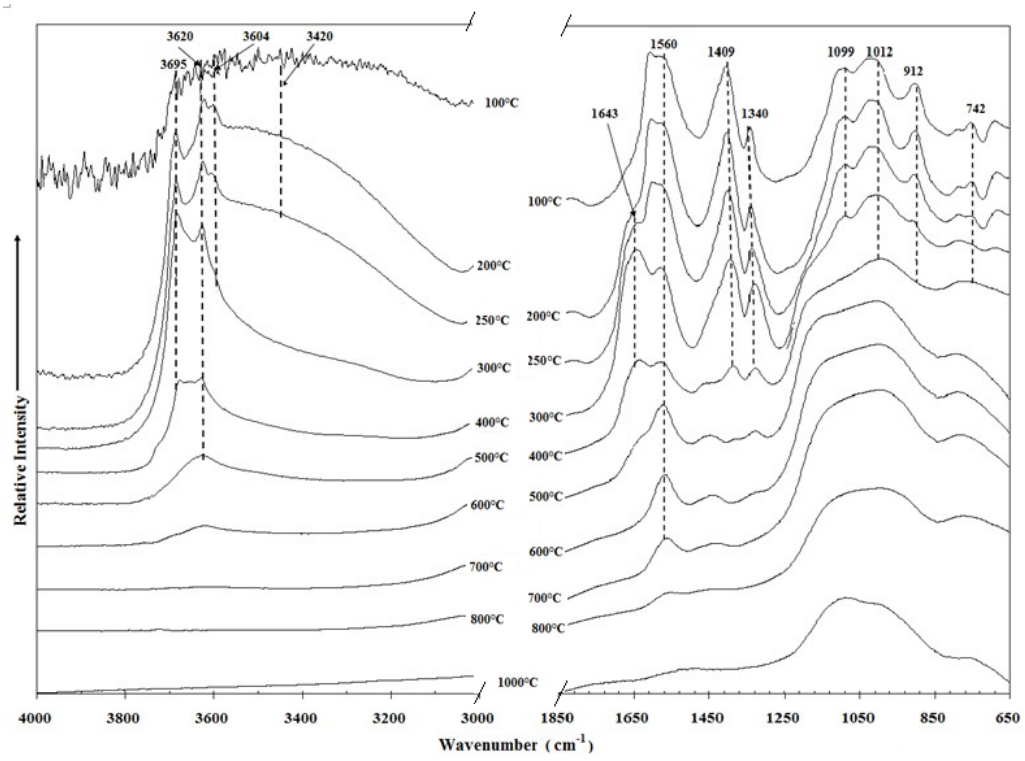
3620
3604
3420
3695
1560
1409
1099
1012
912
1643
1340
742
100°C
200°C
250°C
300°C
400°C
500°C
600°C
700°C
800°C
1000°C
Relative Intensity
4000
3800
3600
3400
3200
3000
1850
1650
1450
1250
1050
850
650
Wavenumber (cm-1)

Fig.7

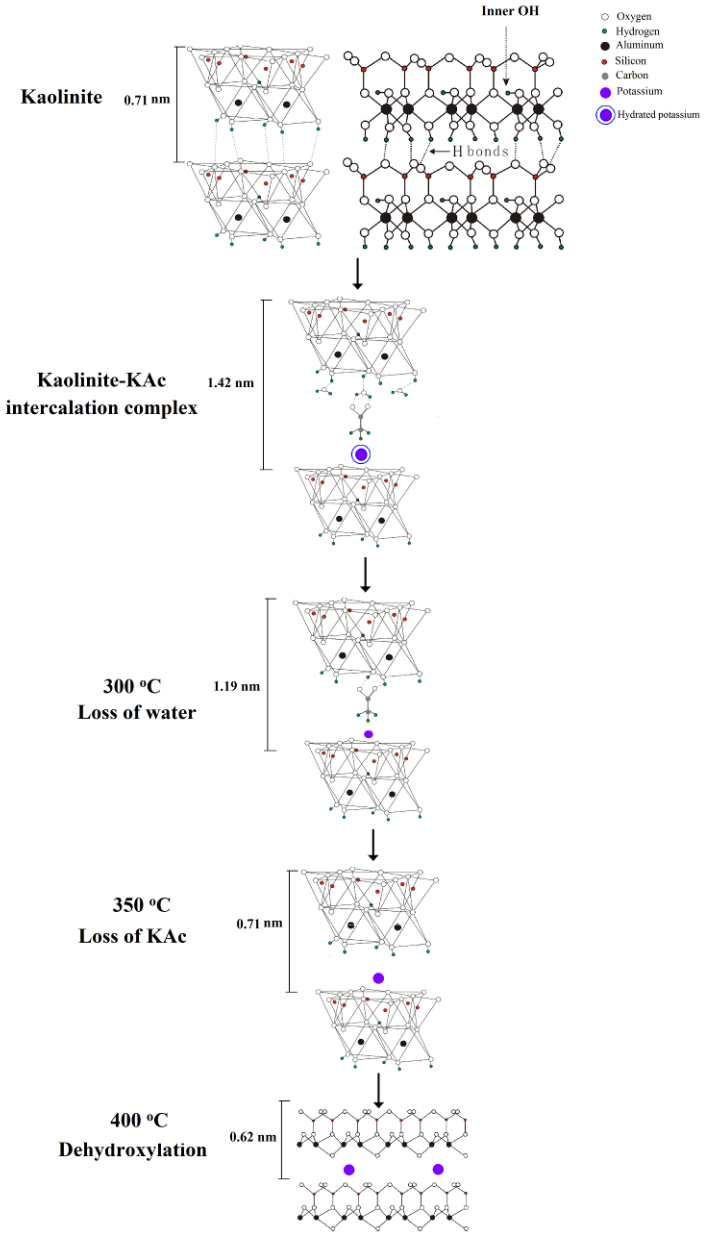
Inner OH
Oxygen
Hydrogen
Aluminum
Silicon
Carbon
Potassium
Hydrated potassium
Kaolinite
0.71 nm
H bonds
Kaolinite-KAc
intercalation complex
1.42 nm
300 °C
Loss of water
1.19 nm
350 °C
Loss of KAc
0.71 nm
400 °C
Dehydroxylation
0.62 nm

Fig. 8